JOURNAL OF MATERIALS SCIENCE **37** (2002) 2885–2891

High temperature strength at 1773 K and room temperature fracture toughness of Nb_{ss}/Nb_5Si_3 *in situ* composites alloyed with Mo

W.-Y. KIM*, H. TANAKA
Japan Ultra-High Temperature Materials Research Institute (JUTEMI), 573-3 Okiube, Ube, Yamaguchi 755-0001, Japan
E-mail: Kim@jutem.co.jp

S. HANADA
Institute for Materials Research, Tohoku University, Sendai 980-8577, Japan

High temperature compressive strength at 1773 K and room temperature fracture toughness have been studied in terms of microstructure, phase stability and solid solution hardening in Nb-Si-Mo *in situ* composites consisting of niobium solid solution and Nb_5Si_3. Molybdenum addition stabilizes the β-Nb_5Si_3 phase and makes unstable Nb_3Si phase in the *in situ* composite. It is found that molybdenum has a strong effect to increase the yield stress of the present *in situ* composite at 1773 K due to solid solution hardening. Yield strength depends not only on chemical composition and volume fraction but also the Nb_5Si_3 phase itself. Room temperature fracture toughness is very sensitive to microstructure and the content of ternary alloying element, but not to the volume fraction of constituent phases within the composition ranges investigated. It is suggested that plastic deformation of Nb solid solution and interface decohesion is responsible for high fracture toughness in this alloy system. Details are discussed in relation to microstructural features and Molybdenum alloying.

1. Introduction

Refractory metal silicides are currently being considered for one of potential candidates to use at ultra-high temperature beyond those presently attainable with nickel-based superalloys. Among those alloy systems, Nb-Si alloy system is of our interest because of its wide two-phase region consisting of a ductile Nb solid solution (Nb_{ss}) and Nb_5Si_3 intermetallic phase, which melting point is about 2527 K [1]. So, high temperature strength can be anticipated by the intermetallic phase, and low temperature fracture toughness can be achieved by an incorporated Nb_{ss} phase since monolithic Nb_5Si_3 phase has been found to have very low fracture toughness at room temperature (3 MPa $m^{1/2}$, [2, 3]). It has also been demonstrated that the fracture resistance of Nb_{ss}/Nb_5Si_3 *in situ* composites is superior to the single Nb_5Si_3 intermetallic phase in the binary Nb-Si system due to ductile phase toughening base mechanisms [2–8]. Extensive studies have been carried out to clarify the toughening mechanisms, and to understand the role of ductile phase on the fracture toughness or fatigue crack propagation in some Nb-base *in situ* composites [2–12]. Ashby *et al*. [13] have been proposed that fracture toughness for composite material in which microstructure is composed of hard matrix phase and ductile reinforcement is given by

$$K_c = K_m + E[CV_f(\sigma_0/E)a_0]^{1/2}$$

where, K_m is the fracture toughness of matrix, and E is the elastic modulus, V_f is volume fraction, σ_0 is the yield strength, and a_0 is radius or thickness, of the ductile phase. The parameter C is a constant required to rupture the ductile phase. Substantially, fracture toughness of *in situ* composites would be largely dependent on the volume fraction of constituent phases and microstructure. Therefore, it would be expected that the *in situ* composites having large volume fraction of ductile phase could be favorable for room temperature fracture toughness. Under such phase combinations, however, poor high temperature strength may result due to low strength of Nb_{ss} at high temperature in binary composites. In the present study, we chose Mo as a ternary alloying element due to its high melting point, phase stability and solid solution hardenability in the Nb_{ss}/Nb_5Si_3 *in situ* composites. Moreover, various processing techniques are employed to modify the microstructure in relation with high temperature strength at 1773 K and room temperature fracture toughness.

2. Experimental procedure

The raw materials used in the present study were 99.9 wt% of Nb, 99.999 wt% of Si and 99.9 wt% of

*Author to whom all correspondence should be addressed.

TABLE I The nominal compositions (by at.%) and microstructural characteristics of alloys used in this study

Sample no.	Nb	Si	Mo	Constituent phases	V_f of Nb_{ss} (V_f)	Thickness of Nb_{ss} (μm)	Processing/Heat treatment
Alloy a	67	18	15	Nb_{ss} and α-Nb_5Si_3	55	4.1	Arc-melting/1973 K for 48 h.
Alloy b	67	18	15	Nb_{ss} and β-Nb_5Si_3	55	4.8	Arc-melting/2123 K for 48 h.
Alloy c	67	18	15	Nb_{ss} and α-Nb_5Si_3	55	4.8	Arc-melting/1973 K for 48 h after heat treated at 2123 K for 48 h.
Alloy d	67	18	15	Nb_{ss} and α-Nb_5Si_3	55	1.6	DS/1973 K for 48 h.
Alloy e	69	16	15	Nb_{ss} and β-Nb_5Si_3	62	9.1	Arc-melting/2123 K for 48 h.
Alloy f	63	22	15	Nb_{ss} and β-Nb_5Si_3	43	5.1	Arc-melting/2123 K for 48 h.
Alloy g	77	18	5	Nb_{ss} and α-Nb_5Si_3	55	7.1	Arc-melting/2123 K for 48 h.

Mo. Various Nb_{ss}/Nb_5Si_3 *in situ* composites were produced in this study. Alloy buttons were prepared under an argon gas atmosphere on a copper hearth with non-consumable tungsten electrode. The alloy buttons melted were turned over and re-melted at least 3 times to ensure chemical homogeneity. The growth of a bulk DS (directional solidification) crystal with about 10 mm diameter was carried out using floating zone technique in an induction furnace. The compositions by chemical analysis after heat treatment are in good agreement with the nominal compositions. Heat treatment of arc-melted alloy buttons and DS alloys for homogenization was conducted at 1973 K and at 2123 K followed by furnace rapid cooling. The nominal compositions and microstructural characteristics of some ternary alloys used in this study are listed in Table I. Microstructure and fractographic observations were undertaken using optical microscope (OM), scanning electron microscope (SEM). X-ray diffraction (XRD) analysis was performed on the bulk samples with fine final polishing. Compression specimens with 2.5×2.5 mm cross-section and 6 mm height and fracture toughness specimens with 3×6 mm cross-section with 24 mm span were mechanically polished using SiC paper and Al_2O_3 particles with water. Compression tests were carried out using an Instron model 8500 mechanical testing machine under an argon atmosphere at 1773 K and at an initial strain rate of 3×10^{-4} s^{-1}. Fracture toughness test was carried out on notched three point bending specimens without insertion of a fatigue initial crack at room temperature. Fracture toughness tests were

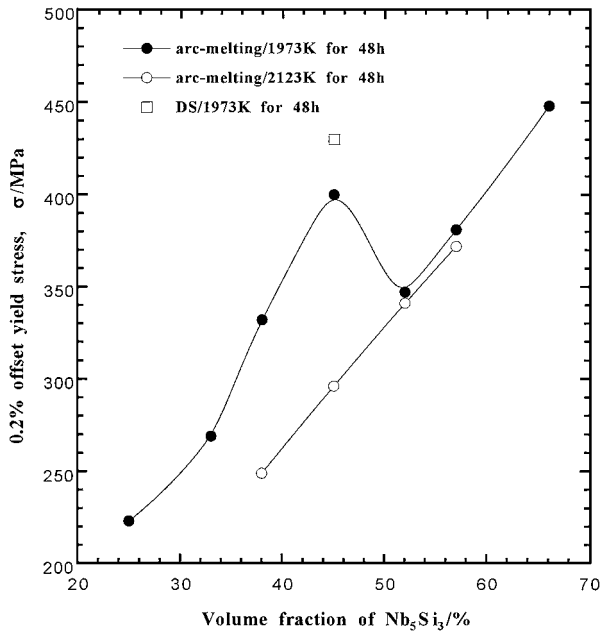

Figure 1 The 0.2% offset yield stress as a function of volume fraction of Nb_5Si_3 for three kinds of alloys in the Nb-Si-Mo ternary alloy system.

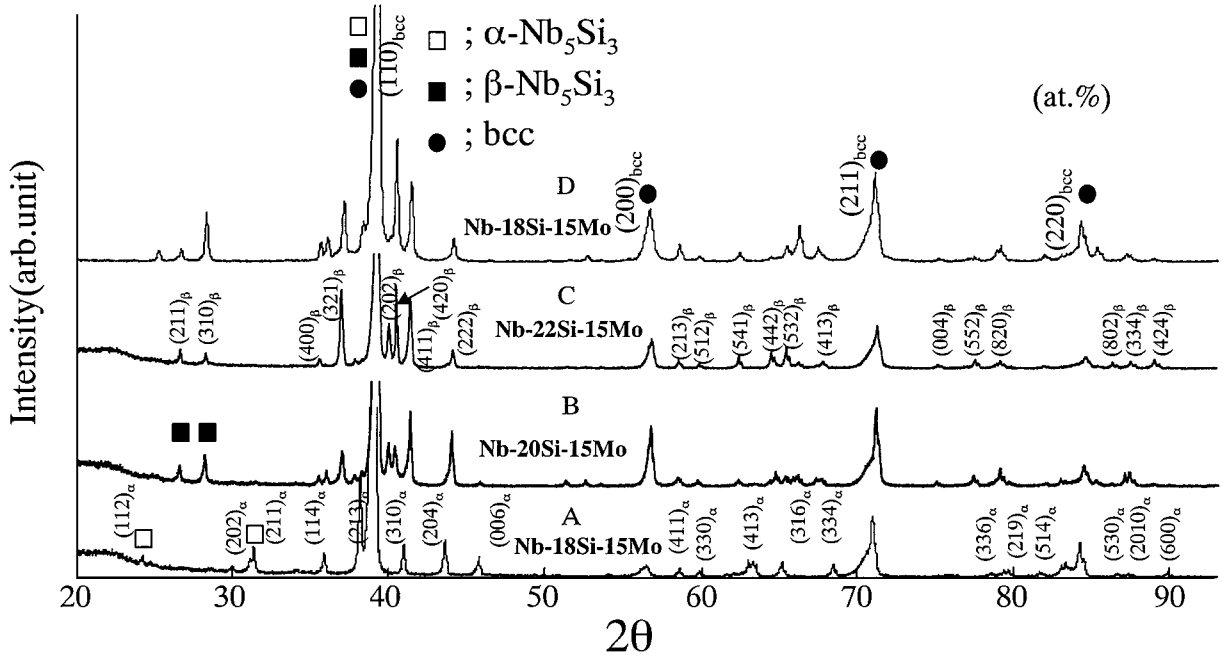

Figure 2 XRD spectra for four two-phase alloys heat treated at 1973 K (a, b, c) and at 2123 K (d).

performed in air at room temperature and at a cross-head speed of 0.5 mm/min.

3. Results and discussion

The variation of yield stress for the Mo-added ternary *in situ* composites plotted as a function of volume fraction of Nb_5Si_3 phase is presented in Fig. 1. Yield stresses increased with increasing volume fraction of Nb_5Si_3 but exhibited a sudden decrease at 52% of Nb_5Si_3 phase and then increased again with further increasing volume fraction of Nb_5Si_3 in the alloys heat treated at 1973 K. In the alloys heat treated at 2123 K,

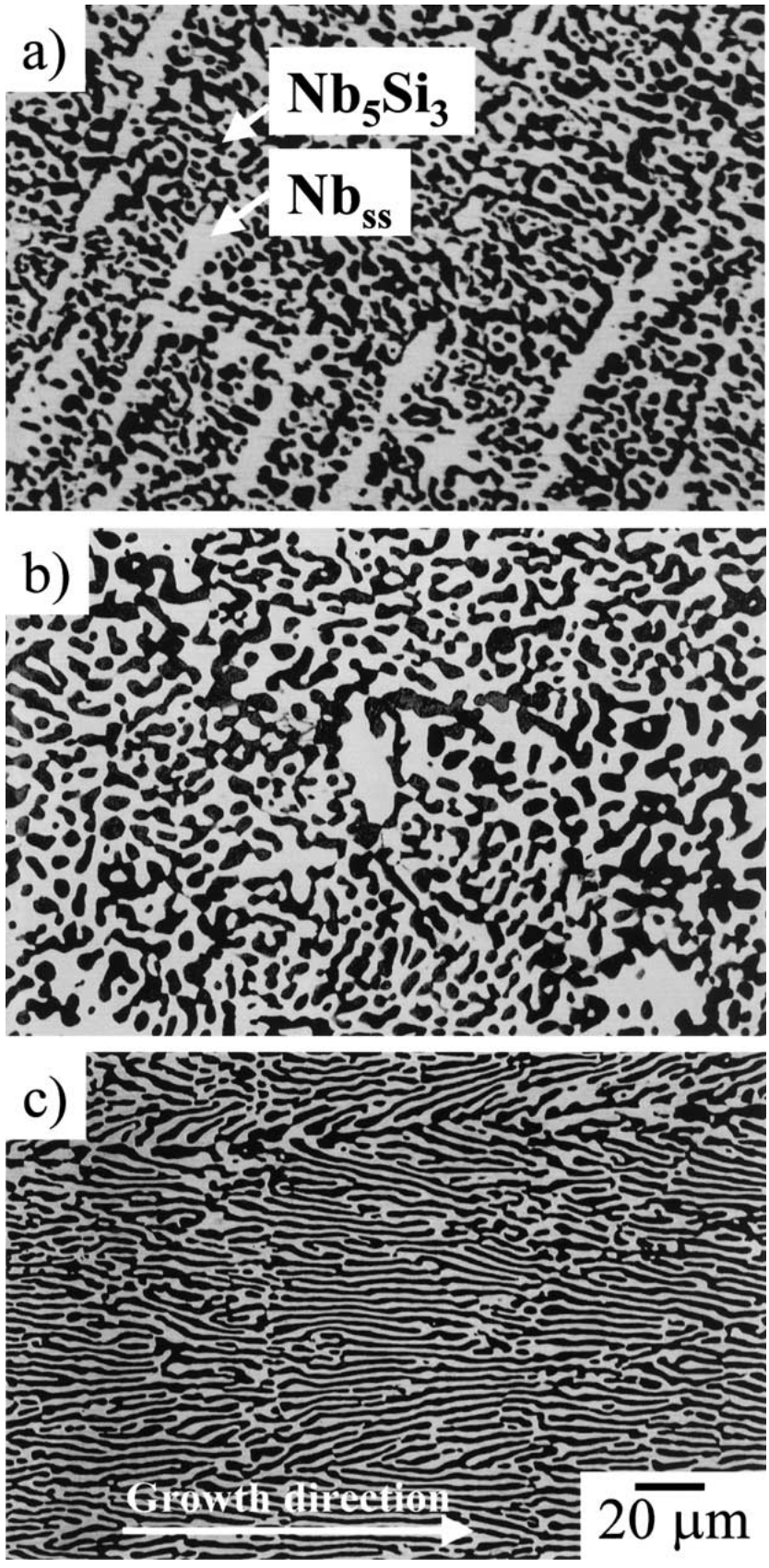

Figure 3 Optical micrographs of the microstructures of Nb-18at.%Si-15at.%Mo alloy heat treated at 1973 K for 48 h (a, c) and 2123 K for 48 h (b). Note that the microstructure (a) and (b) are produced by arc melting, and the (c) is produced by DS processing in this figure.

however, no such yield stress drop is observed over the whole volume fraction range investigated. It is interesting to note that the discrepancy in yield stress between the alloys heat treated at 1973 K and the ones heat treated at 2123 K is observed only in the volume fraction range of alloys less than about 50% of Nb_5Si_3 through the whole alloys. The yield stresses obtained in the alloys containing the volume fraction more than about 50% of Nb_5Si_3 are appeared to be insensitive to heat treatment temperature, that is, similar yield stress. While, it is observed that the yield stress of the alloy produced by DS (aligned microstructure) is slightly higher but not so much. The results of X-ray diffraction on several samples heat treated at both 1973 K and 2123 K are shown in Fig. 2. The data points shown as open-squares in the figure indicate peaks due to the α-Nb_5Si_3, and the closed-circles indicate peaks from the bcc solid solution. The β-Nb_5Si_3 phase is marked by closed-squares. Whilst most diffraction peaks are common to the two Nb_5Si_3 phases, the 112 and 202 peaks of the α-Nb_5Si_3 phase and the 211 and 310 peaks of the β-Nb_5Si_3 phase allow their presence to be uniquely determined. We could not find an intermediate Nb_3Si phase in the present alloys whatever heat treatment was performed at 1973 K or 2123 K. Therefore Mo additions to the Nb_5Si_3/Nb_{ss} *in situ* composite appears to make Nb_3Si unstable since the Nb_3Si phase exists as an intermediate phase in the binary Nb-Si phase diagram [1]. It has been found that the phase transformation from α-Nb_5Si_3 to β-Nb_5Si_3 occurs at the Mo content of about 5at.% for Mo-added Nb_{ss}/Nb_5Si_3 alloys heat treated at 1973 K and which exhibits a dependence of chemical composition [14]. In contrast, no compositional dependence for the occurrence of phase transformation is observed in the alloy heat treated at 2123 K. By XRD results, all the *in situ* composites heat treated at 2123 K are revealed to be composed of β-Nb_5Si_3 and Nb_{ss} within the composition range investigated in this study. The yield stress drop shown in Fig. 1, therefore can be closely associated with the occurrence of phase transformation from α to β, indicating a higher strength of α-Nb_5Si_3 than β-Nb_5Si_3 at 1773 K. Regarding the effect of microstructure on yield stress, similar values are obtained in the present alloys when the constituting phases were not changed by heat treatment at the same chemical composition. Back scattering electron images (BEI) of Nb-18at.%Si-15at.%Mo (hereafter denoted as Nb-18Si-15Mo) alloys with various microstructures produced by arc melting (a, b) and DS (c) are shown in Fig. 3. The heat treatment of the alloys was carried out at 1973 K (a, c) and at 2123 K (b) to verify microstructures and constituent intermetallic Nb_5Si_3 phases. The lightly and darkly contrasted regions as indicated arrows in the Fig. 3 correspond to Nb_{ss} and Nb_5Si_3 phase, respectively. The microstructure for the DS alloy is observed to have a fine and aligned Nb_{ss} structure with 1.6 μm in thickness along the crystal growth direction. While the microstructure produced by arc melting and heat treatment is characterized as a maze-like structure composed of primary Nb_{ss} and a eutectic. The microstructure of the Nb_{ss} phase appears to coarse with increasing heat treatment temperature as seen in Fig. 3a and b. With respect to the volume fraction, no change is found by a variation of processing from *alloy a* to *alloy d* at constant Si content, since the volume fraction of each of constituent phases has been reported to be a strong function of Si content in this alloy system [14]. Microstructural characteristics together with nominal composition of the present alloys are summarized in Table I. Room temperature fracture toughness values of various ternary alloys plotted as a function of microstructure and chemical composition are shown in Figs 4 and 5, respectively. Concerning the effect of microstructure as shown in Fig. 4, the fracture toughness values of arc-melted alloys are obtained

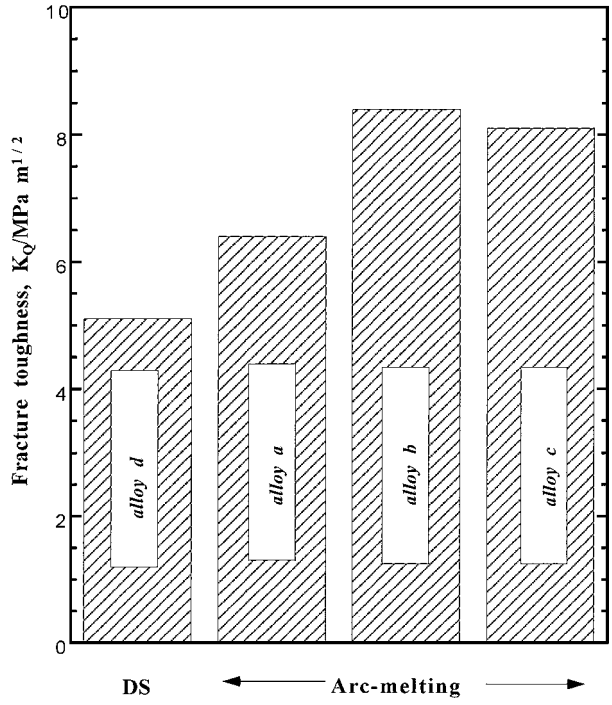

Figure 4 Effect of microstructure on room temperature fracture toughness the Nb-Si-Mo ternary alloy system.

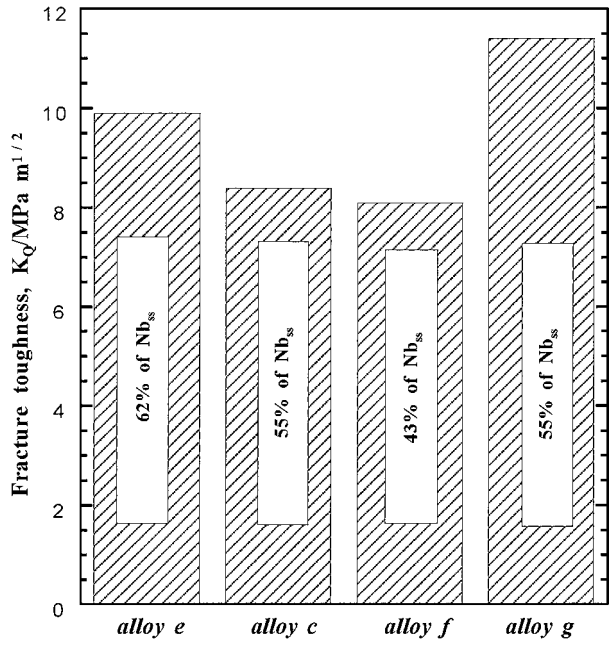

Figure 5 Effect of volume fraction and chemical composition on room temperature fracture toughness the Nb-Si-Mo ternary alloy system.

to be higher than DS alloy although an aligned microstructure to the perpendicular of testing direction is evolved in the DS alloy. Moreover, higher fracture toughness is attained in the *alloy b* with coarser microstructure (4.8 μm in thickness of Nb_{ss}) than the *alloy a* (4.1 μm in thickness of Nb_{ss}). While, in relation with the effect of the silicide phase equilibrated with Nb_{ss}, it is observed that there is no significant difference in fracture toughness between the *alloy b* (Nb_{ss}/β-Nb_5Si_3) and *alloy c* (Nb_{ss}/α-Nb_5Si_3), even though β-Nb_5Si_3 has

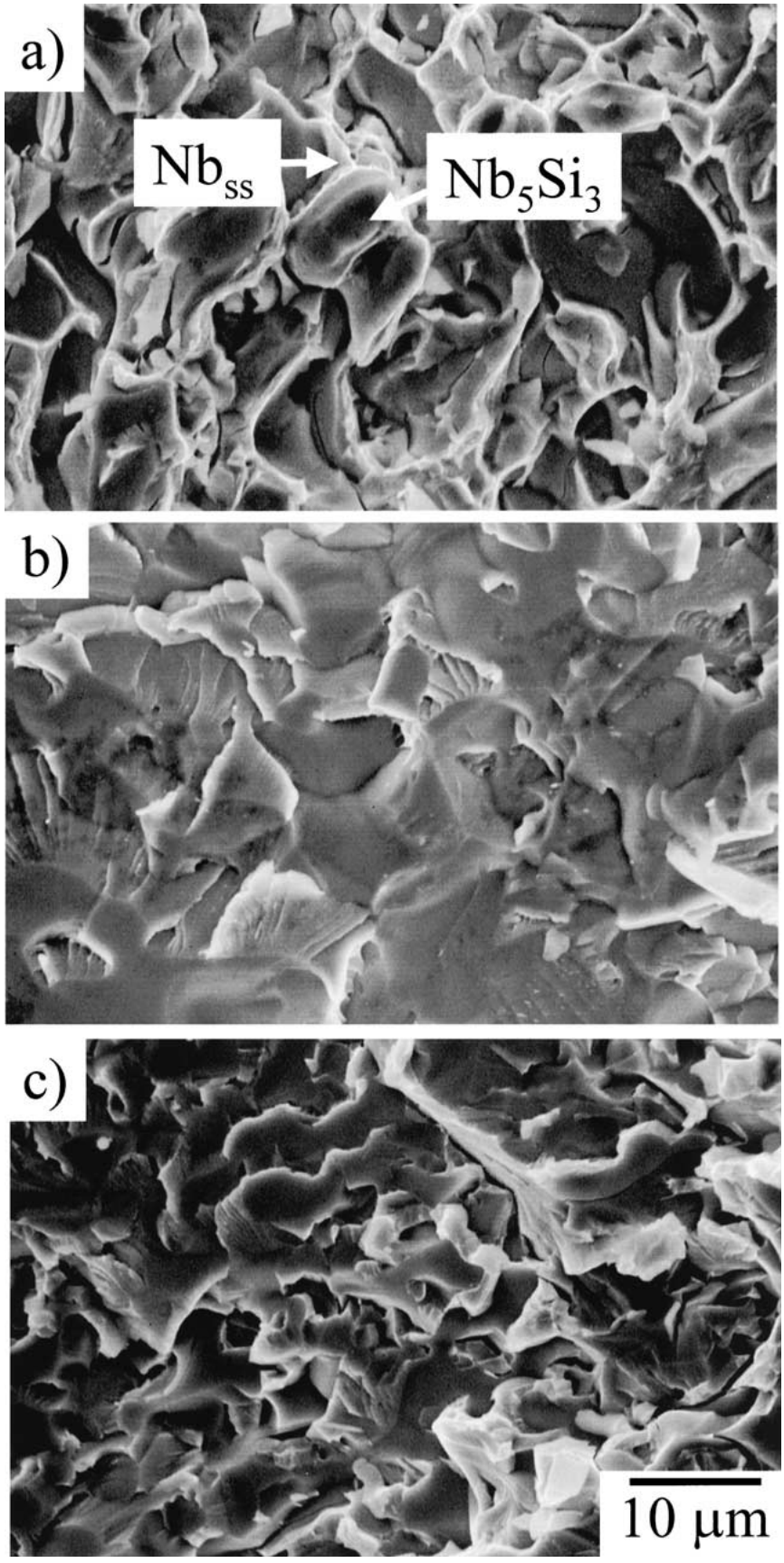

Figure 6 SEM fractographs of (a) Nb-18at.%Si-5at.%Mo (b) Nb-18at.%Si-15at.%Mo (c) Nb-22at.%Si-15at.%Mo alloys produced by arc melting and then heat treatment at 2123 K for 48 h.

a better deformability from the compression results as shown in Fig. 1. These results suggest that the thickness and morphology of an incorporated ductile bcc phase play an important role to enhance the fracture toughness in this alloy system. Fracture toughness plotted as a function of chemical composition to understand the effect of volume fraction and ternary alloying element is presented in Fig. 5. Concerning the effect of volume fraction, Nb-16Si-15 Mo (*alloy e*) with 62% of Nb_{ss} showed a slightly higher value of fracture toughness compared to the Nb-18Si-15Mo (*alloy c*) with 55% of Nb_{ss} and Nb-22Si-15Mo (*alloy f*) with 43% of Nb_{ss} at the same content of Mo. However, similar fracture toughness values are observed for both *alloy c* and *alloy f* even though *alloy c* has a large volume fraction of Nb_{ss} than *alloy f*. One possible explanation for this result is that no remarkable difference in thickness of Nb_{ss} is observed on both *alloy c* (4.8 μm) and *alloy f* (5.1 μm) if we assume that similar fracture mechanisms are operating at both alloys. From these results, it may imply that microstructural control is much effective in enhancing fracture thoughness than volume fraction control within the compositional range investigated in this study. If the improvement of fracture toughness is associated with this volume fraction and thickness of Nb_{ss}, thicker Nb_{ss} and larger volume fraction should improve the fracture toughness. Nevertheless *alloy g* with 55% of Nb_{ss} exhibited higher fracture toughness than *alloy e* with 62% of Nb_{ss}. Furthermore, *alloy g* has a thinner Nb_{ss} (7.1 μm) than *alloy e* (9.1 μm), as listed in Table I. These results indicate that in addition to above factors described, the effect of Mo content, which is closely related to the solid solution hardening of Nb_{ss} phase, should be considered in understanding fracture toughness results. As the Mo content is increased, the strength at temperatures ranging from room temperature to high temperature has been found to be increased [15], however, ductility has been reported to be decreased at room temperature [16]. A potential positive implication is that room temperature ductility rather than strength should be considered in improving fracture toughness via various toughening mechanisms in the present Nb_{ss}/Nb_5Si_3 *in situ* composites alloyed with Mo. Fracture surfaces of Nb-18Si-5Mo, Nb-18Si-15Mo and Nb-22Si-15Mo alloys are shown in Fig. 6. All alloys in this figure are produced by arc melting and then heat treatment at 2123 K for 48 h. In Nb-18Si-5Mo the Nb_{ss} surrounding Nb_5Si_3 exhibits a fibrous pattern and decohesion is seen at Nb_{ss}/Nb_5Si_3 interfaces, while the Nb_5Si_3 phase fractures in a brittle manner completely as indicated by arrow in the Fig. 6. In Nb-18Si-15Mo a plastic stretching of Nb_{ss} is not evidenced clearly, however, the interface decohesion between Nb_{ss} and Nb_5Si_3 phase is frequently observed. A similar fracture appearance is also observed in the Nb-22Si-15Mo. Therefore, it is suggested that dominant plastic stretching of Nb_{ss} and decohesion can be a potent toughening mechanism when the incorporated Nb_{ss} is sufficiently ductile. On the other hand, interface decohesion can be operative as a toughening mechanism when the incorporated Nb_{ss} is insufficiently ductile. From these viewpoints of fracture toughness, it is suggested that a control of microstructures such as morphology and thickness of Nb_{ss} as well as solid solution hardening is essential in enhancing fracture toughness of Nb_{ss}/Nb_5Si_3 *in situ* composites. On the basis of the present results obtained, it is suggested that coarse microstructures consisting of thick Nb_{ss} and α-Nb_5Si_3 is expected to have a good balance for the both viewpoints of high temperature strength and room temperature fracture toughness in Nb_{ss}/Nb_5Si_3 *in situ* composites alloyed with Mo. Much more work will be required to clarify the effects of interfaces between Nb_{ss} and Nb_5Si_3 on both high temperature strength and room temperature fracture toughness in this alloy system.

4. Conclusions

High temperature strength at 1773 K and room temperature fracture toughness of Nb_{ss}/Nb_5Si_3 *in situ* composites alloyed with Mo are investigated in terms of volume fraction of constituent phases and microstructures produced by various processing. The yield strength of the present *in situ* composites is dependent not only on the volume fraction of constituent phase but also on the intermetallic Nb_5Si_3 phase itself. The *in situ* composites consisting of Nb_{ss} and α-Nb_5Si_3 showed higher strength than those alloys consisting of Nb_{ss} and β-Nb_5Si_3. The maze-like microstructure with thick Nb_{ss} provided by arc melting is appeared to be favorable for the room temperature fracture toughness than the aligned microstructure created by DS. From these results, it is proposed that coarse microstructures with thick Nb_{ss} and α-Nb_5Si_3 are desirable for the combination of high temperature strength and room temperature fracture toughness in Nb_{ss}/Nb_5Si_3 *in situ* composites alloyed with Mo.

Acknowledgment

This work is supported by a grant from the New Energy and Industrial Technology Development Organization (NEDO) of Japan.

References

1. T. B. MASSALSKI (ed.), "Binary Alloy Phase Diagram" Vol. 2 (ASM, Metals Park, OH, 1986).
2. R. M. NEKKANTI and D. M. DIMIDUK, in "MRS. Symp. Proc. on Intermetallic Composites," edited by D. Miracle, J. Graves and D. L. Anton (MRS, PA, 1990) p. 349.
3. J. KAJUCH, J. SHORT and J. J. LEWANDOWSKI, *Acta Metal. Mater.* **43** (1995) 1955.
4. M. G. MENDIRATTA, J. J. LEWANDOWSKI and D. M. DIMIDUK, *Metall. Trans.* A **22A** (1991) 1573.
5. M. G. MENDIRATTA and D. M. DIMIDUK, *Metall. Trans.* A **24A** (1993) 501.
6. J. D. RIGNEY, P. M. SINGH and J. J. LEWANDOWSKI, *JOM* **44**(8) (1992) 36.
7. K. S. CHAN, *Metall. Trans.* A **27A** (1996) 2518.
8. J. J. LEWANDOWSKI, D. M. DIMIDUK and M. G. MENDIRATTA, in MRS. Symp. Proc., Vol. 20, edited by F. D. Lemkey, A. G. Evans, S. G. Fishman and J. R. Strife (MRS, PA, 1988) p. 103.
9. D. L. ANTON and D. M. SHAW, in "MRS. Symp. Proc. on Intermetallic Matrix Composites," edited by D. L. Anton, R. McMeeking, D. Miracle and P. Martin (MRS, PA, 1989) p. 45.
10. R. GNANAMOORTY and S. HANADA, *Scripta Mater.* **34** (1996) 999.

11. J. KAJUCH and J. J. LEWANDOWSKI, *Mater. Sci. Eng.* A **A155** (1992) 59.
12. J. D. RIGNEY and J. J. LEWANDOWSKI, *Metal. Trans.* A **27A** (1991) 3292.
13. M. F. ASHBY, F. L. BLUNT and M. BANNISTER, *Acta Metall Mater.* **37** (1989) 1847.
14. W.-Y. KIM, H. TANAKA, A. KASAMA, R. TANAKA and S. HANADA, *Intermetallics* **9** (2001) 521.
15. E. MIURA, K. YOSHIMI and S. HANADA, *Phy. Stat. Sol(a).*, in press.
16. N. NAKAO, Master thesis, Tohoku University, 1996.

Received 14 August 2001
and accepted 9 April 2002